The influence of defects formed by Ca excess and thermal post-treatments on the persistent luminescence of $CaTiO_3$:Pr

Eugenio H. Otal,[1] Alexandra E. Maegli,[1] Nina Vogel-Schäuble,[1] Bernhard Walfort,[2] Hans Hagemann,[3] Songhak Yoon,[1] Albert Zeller,[2] and Anke Weidenkaff[1,*]

[1]*Empa, Swiss Federal Laboratories for Materials Science and Technology, Laboratory for Solid State Chemistry and Catalysis, Ueberlandstrasse 129, CH-8600 Dübendorf, Switzerland*
[2]*LumiNova AG, Speicherstrasse 60A, CH-9053 Teufen, Switzerland*
[3]*Département de Chimie Physique, Univ. de Genève, 30, quai E. Ansermet, CH-1211 Geneva 4, Switzerland*
**anke.weidenkaff@empa.ch*

Abstract: Red emitting $CaTiO_3$:Pr phosphors with a nominal composition of $Ca_{0.998+x}Pr_{0.002}TiO_{3+\delta}$ ($0.02 \leq x \leq 0.04$) were prepared by solid state reactions with different thermal post treatments and characterized by X-ray diffraction, transmission electron microscopy and photoluminescence. The Ca excess exhibited complete solubility up to 4% in the samples treated at 1400 °C but segregation in the form of Ruddlesden-Popper phases ($Ca_3Ti_2O_7$ - $Ca_4Ti_3O_{10}$) was observed in samples prepared at 1500 °C. The increase in temperature for stoichiometric samples showed a monotonic increase of decay time due to the reduction of non-radiative recombination defects. It was found that the Ca excess favored the formation of oxygen vacancies which are known to act as trap. In the samples treated at 1400 °C, 3% of Ca excess showed to be the best concentration to increase the decay time of persistent luminescence. For the samples treated at 1500 °C, the segregation of Ruddlesden-Popper phases left a constant amount of Ca soluble in all the $CaTiO_3$ samples. This constant concentration of Ca caused the same density of defects and, consequently, the same decay time in all samples.

OCIS codes: (160.4760) Optical properties; (160.5690) Rare-earth-doped materials; (160.2540) Fluorescent and luminescent materials.

References and links

1. T. Matsuzawa, "A new long phosphorescent phosphor with high brightness, $SrAl_2O_4:Eu^{2+},Dy^{3+}$," J. Electrochem. Soc. **143**(8), 2670–2673 (1996).
2. Y. Lin, Z. Tang, and Z. Zhang, "Preparation of long-afterglow $Sr_4Al_{14}O_{25}$-based luminescent material and its optical properties," Mater. Lett. **51**(1), 14–18 (2001).
3. P. F. Smet, N. Avci, and D. Poelman, "Red persistent luminescence in Ca_2SiS_4:Eu,Nd," J. Electrochem. Soc. **156**(4), H243–H248 (2009).
4. X. Wang, Z. Zhang, Z. Tang, and Y. Lin, "Characterization and properties of a red and orange Y_2O_2S-based long afterglow phosphor," Mater. Chem. Phys. **80**(1), 1–5 (2003).
5. A. Lecointre, A. Bessière, A. J. J. Bos, P. Dorenbos, B. Viana, and S. Jacquart, "Designing a red persistent luminescence phosphor: the example of $YPO_4:Pr^{3+},Ln^{3+}$ (Ln = Nd, Er, Ho, Dy)," J. Phys. Chem. C **115**(10), 4217–4227 (2011).
6. D. Jia, W. Jia, D. R. Evans, W. M. Dennis, H. Liu, J. Zhu, and W. M. Yen, "Trapping processes in $CaS:Eu^{2+},Tm^{3+}$," J. Appl. Phys. **88**(6), 3402–3407 (2000).
7. X.-J. Wang, D. Jia, and W. M. Yen, "Mn^{2+} activated green, yellow, and red long persistent phosphors," J. Lumin. **102–103**, 34–37 (2003).
8. X.-B. Yu, L.-H. Mao, L.-Z. Zhang-Fan, L.-Z. Yang, and S.-P. Yang, "The synthesis of $ZnS:Mn^{2+}$ nano-particles by solid-state method at low temperature and their photoluminescence characteristics," Mater. Lett. **58**(29), 3661–3664 (2004).
9. K. Van den Eeckhout, P. F. Smet, and D. Poelman, "Persistent luminescence in rare-earth codoped $Ca_2Si_5N_8:Eu^{2+}$," J. Lumin. **129**(10), 1140–1143 (2009).
10. Y. Pan, Q. Su, H. Xu, T. Chen, W. Ge, C. Yang, and M. Wu, "Synthesis and red luminescence of Pr^{3+}-doped $CaTiO_3$ nanophosphor from polymer precursor," J. Solid State Chem. **174**(1), 69–73 (2003).

#160080 - $15.00 USD Received 19 Dec 2011; revised 1 Mar 2012; accepted 2 Mar 2012; published 7 Mar 2012

11. S. S. Chedha, D. W. Smith, A. Vecht, and C. S. Gibbons, "New and improved phosphors for low-voltage applications," SID Int. Symp. Digest Tech. Papers **51**, 51–54 (1994).
12. W. Jia, D. Jia, T. Rodriguez, D. R. Evans, R. S. Meltzer, and W. M. Yen, "UV excitation and trapping centers in $CaTiO_3:Pr^{3+}$," J. Lumin. **119–120**, 13–18 (2006).
13. S. M. Jacobsen, "Phosphors for full-color low-voltage field-emission displays," J. Soc. Inf. Disp. **4**, 331–335 (1996).
14. J.-C. Zhang, X. Wang, and X. Yao, "Enhancement of luminescence and afterglow in $CaTiO_3:Pr^{3+}$ by Zr substitution for Ti," J. Alloy. Comp. **498**(2), 152–156 (2010).
15. S. Yin, D. Chen, and W. Tang, "Combustion synthesis and luminescent properties of $CaTiO_3$: Pr, Al persistent phosphors," J. Alloy. Comp. **441**(1-2), 327–331 (2007).
16. X. Zhang, J. Zhang, X. Zhang, L. Chen, S. Lu, and X.-J. Wang, "Enhancement of red fluorescence and afterglow in $CaTiO_3$: Pr^{3+} by addition of Lu_2O_3," J. Lumin. **122–123**, 958–960 (2007).
17. X. Zhang, J. Zhang, X. Zhang, M. Wang, H. Zhao, S. Lu, and X. Wang, "Size manipulated photoluminescence and phosphorescence in $CaTiO_3:Pr^{3+}$ nanoparticles," J. Phys. Chem. C **111**(49), 18044–18048 (2007).
18. M. F. Zhou, T. Bak, J. Nowotny, M. Rekas, C. C. Sorrell, and E. R. Vance, "Defect chemistry and semiconducting properties of calcium titanate," J. Mater. Sci. Mater. Electron. **13**(12), 697–704 (2002).
19. A. Zhu, J. Wang, D. Zhao, and Y. Du, "Native defects and Pr impurities in orthorhombic $CaTiO_3$ by first-principles calculations," Physica B **406**(13), 2697–2702 (2011).
20. M. Čeh and D. Kolar, "Solubility of CaO in $CaTiO_3$," J. Mater. Sci. **29**(23), 6295–6300 (1994).
21. M. M. Elcombe, E. H. Kisi, K. D. Hawkins, T. J. White, P. Goodman, and S. Matheson, "Structure determinations for $Ca_3Ti_2O_7$, $Ca_4Ti_3O_{10}$, $Ca_{3.6}Sr_{0.4}Ti_3O_{10}$ and a refinement of $Sr_3Ti_2O_7$," Acta Crystallogr. B **47**(3), 305–314 (1991).
22. U. Balachandran and N. G. Eror, "Electrical conductivity in calcium titanate with excess CaO," Mater. Sci. Eng. **54**(2), 221–228 (1982).
23. S. N. Ruddlesden and P. Popper, "The compound $Sr_3Ti_2O_7$ and its structure," Acta Crystallogr. **11**(1), 54–55 (1958).
24. B. V. Beznosikov and K. S. Aleksandrov, "Perovskite-like crystals of the Ruddlesden-Popper series," Crystallogr. Rep. **45**(5), 792–798 (2000).
25. W. Kwestroo and H. A. M. Paping, "The systems $BaO-SrO-TiO_2$, $BaO-CaO-TiO_2$, and $SrO-CaO-TiO_2$," J. Am. Ceram. Soc. **42**(6), 292–299 (1959).
26. S. Okamoto and H. Yamamoto, "Emission from $BaTiO_3:Pr^{3+}$ controlled by ionic radius of added trivalent ion," J. Appl. Phys. **91**(8), 5492–5494 (2002).

1. Introduction

The development of new persistent luminescent phosphors for solid state lighting applications is an important field of research due to its commercial applications in the area of safety illumination and emergency signage. These new materials should have efficient energy to light conversion, being environmentally friendly and economically sustainable. On the basis of these requirements, oxide based phosphors are good candidates for the implementation in devices. The most efficient materials for persistent luminescence are in the blue-green region, such as $SrAl_2O_4:Eu^{2+},Dy^{3+}$ [1] and $Sr_4Al_{14}O_{25}:Eu^{2+},Dy^{3+}$ [2], but so far only a few reports for efficient materials in the orange-red region have been found: $Ca_2SiS_4:Eu^{+3},Dy^{+2}$ [3], $Y_2O_2S:Eu^{3+},Mg^{2+},Ti^{4+}$ [4], $YPO_4:Pr^{3+},Ho^{3+}$ [5], $CaS:Eu^{2+},Tm^{3+}$ [6], $MgSiO_3:Eu^{2+},Mn^{2+},Dy^{3+}$ [7], $ZnS:Mn^{2+}$ [8], $Ca_2Si_4N_8:Eu^{2+}$ [9] and $CaTiO_3:Pr^{3+}$ [10]. $CaTiO_3:Pr^{3+}$ is an excellent candidate because the transition $^1D_2 - {}^3H_4$ at 615 nm is close to the "ideal red" (chromaticity coordinates x = 0.680 and y = 0.311) according to the International Commission on Illumination (CIE) [11]. Also its moderate intrinsic conductivity [12] and resistance to high-density electron irradiation [13] make it ideal for its use in flat panel displays (FPD).

Several studies were performed to understand the luminescent properties in $CaTiO_3$:Pr. Zhang et al. enhanced the luminescence and afterglow with substitution of Ti by Zr due to the change in the lattice symmetry from orthorhombic to pseudo-cubic. Also, this replacement reduces the concentration of Pr^{4+} which acts as a luminescence quencher because Zr has only a +4 valence, making the charge transfer impossible like in the case of Ti: Ti^{+4}-O-Pr^{+3} to Ti^{+3}-O-Pr^{+4} [14]. Yin et al. prepared $CaTiO_3$:(Pr,Al) by a combustion method finding a relationship with the photoluminescence intensity and the H_3BO_3 concentration [15]. Zhang et al. suppressed the non-radiative centers and increased the trap density by addition of Lu_2O_3 [16].

An interesting approach to the problem was developed also by Zhang et al. who manipulated the photoluminescence and phosphorescence by changing the size of $CaTiO_3$:Pr nanoparticles [17]. For nanoparticles, where the surface to volume ratio is higher than in bulk materials, the surface defects play an important role as traps or non-radiative recombination

#160080 - $15.00 USD Received 19 Dec 2011; revised 1 Mar 2012; accepted 2 Mar 2012; published 7 Mar 2012

centers [18]. With thermal annealing the surface of nanoparticles is reduced and therefore also the density of surface defects. The authors found the maximum for luminescence intensity in function of the particle size where the system has the optimal balance between traps and non-radiative recombination centers.

Calcium titanate is a well-known material and the chemistry of defects has been deeply studied [18–21]. The incorporation of CaO excess in the lattice can be achieved by the formation of Ruddlesden-Popper (RP) like defects [22,23]. These defects have the form of CaO interlayers with rock salt structure perpendicular to the c-axis of perovskite blocks [24]. The distribution of these slabs in the $CaTiO_3$ structure is either in the form of isolated defects or grouped with irregular periodicity. These defects are soluble in the $CaTiO_3$ lattice up to 1480 °C. At higher temperature, the segregation of Ruddlesden-Popper phases, $Ca_3Ti_2O_7$ and $Ca_4Ti_3O_{10}$, may occur [25]. Ca excess can also be introduced in the lattice by another mechanism, in this case, the Ca and O are placed in its crystallographic site and Ti and O vacancies are formed [20]. This last mechanism should have a stronger influence on the persistent luminescence because oxygen vacancies can act as traps and increase the decay time [12].

In this work we explored the introduction of defects in a controllable way. These high temperature stable defects allowed reducing the non-radiative recombination centers in the surface of the particles and increasing the decay time for the persistent luminescence. The stability of defects in function of temperature and CaO excess concentration was studied to obtain the optimal conditions.

2. Experimental section

Powder samples of $CaTiO_3$:Pr were synthetized by solid state reaction using $CaCO_3$ (Riedel-de Haën – puriss.), TiO_2 (Sigma Aldrich – puriss.) and Pr_2O_3 (Alpha Aesar - 99.9%). The nominal concentration of Pr was 0.2% in all the samples and the Ca concentration was calculated to give a final composition of $Ca_{0.998+x}Pr_{0.002}TiO_{3+\delta}$ ($0.02 \le x \le 0.04$). The raw materials were mixed in a planetary ball mill with ethanol and ZrO_2 balls. The mixed powders were dried at 100 °C to eliminate the solvent and calcined between 1300 °C and 1500 °C during 24 hs in order to obtain the desired phase.

Powder X-ray diffraction (XRD) was used for the characterization of the samples. The XRD patterns of the products were obtained using a PANalytical X´Pert PRO θ-2θ scan system equipped with Johansson monochromator and a X'Celerator linear detector. The incident X-rays had a wavelength of 1.5406 Å (Cu-$K_{\alpha 1}$). The diffraction patterns were scanned from 20° to 100° (2θ) with an angular step interval of 0.0167°.

The nanostructure and elemental composition were studied by transmission electron microscopy using a JEOL JEM 200 FS TEM/STEM together with energy dispersive X-ray spectroscopy (EDS). Powder samples were dispersed in ethanol and transferred to a copper grid supported with a holey carbon film.

The spectra were measured with a Fluorolog 3-22 Instrument at room temperature with a nominal resolution of 1 nm. For the persistence luminescence measurements, the samples were activated during 1 min with UV light (254 nm). The active area was standardized to 1 cm^2 with an approximate thickness of 3 mm. The decay time was measured in a self-made photometer with a photomultiplier tube (Phototec). For the comparison of the performance of the materials, persistent luminescence decay time, the limit of light perception of the dark-adapted human eye was used as parameter (32 ncd/cm^2).

3. Results and discussion

All the samples treated between 1300 °C and 1500 °C exhibited diffraction patterns with $CaTiO_3$ as main phase (Fig. 1). No detectable impurities like CaO or $Ca(OH)_2$ were found by XRD in the samples treated at 1300 °C and 1400 °C, indicating the complete solubility of CaO in $CaTiO_3$. Samples treated at 1500 °C revealed small impurities which can be identified as $Ca_3Ti_2O_7$ and/or $Ca_4Ti_3O_{10}$. The low intensity and the overlap of the reflexes with the ones corresponding to $CaTiO_3$ made it difficult to clearly identify the phase.

#160080 - $15.00 USD Received 19 Dec 2011; revised 1 Mar 2012; accepted 2 Mar 2012; published 7 Mar 2012

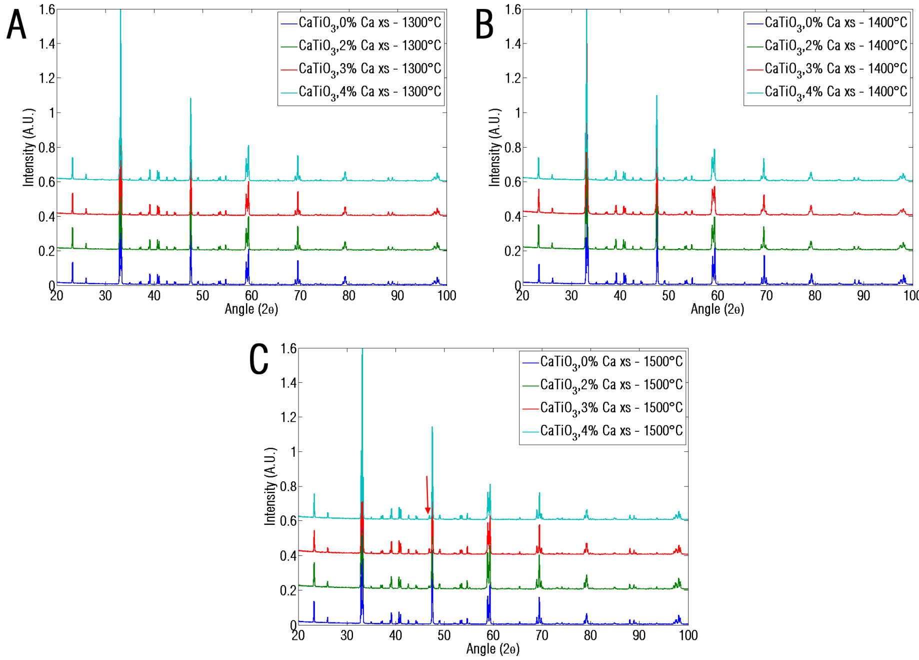

Fig. 1. X-ray diffraction patterns of $CaTiO_3$:Pr samples with different Ca excess treated at (a) 1300 °C, (b) 1400 °C and (c) 1500 °C. The arrow in the last figure indicates the peak corresponding to the RP phase.

The CaO excess can be incorporated in the crystal structure in the form of local defects (Ti and O vacancies) and/or CaO layers (according to the mechanisms mentioned above) when the samples are prepared at 1300 °C and 1400 °C. The existence of $Ca_3Ti_2O_7$ in the samples treated at 1500 °C is in good agreement with the phase diagram reported by Roth [25] in which the formation of the Ca rich phase is observed at 1480 °C.

The local composition of $CaTiO_3$:Pr samples treated at 1400 °C was studied by TEM and EDS. EDS measurements of all samples confirmed the existence of $CaTiO_3$ grains with a Ca:Ti ratio of 1:1. Figure 2 shows a line scan across the particle prepared with 3% Ca excess. The Ca:Ti ratio is close to one, confirming the homogeneous distribution of Ca excess in the $CaTiO_3$ particles.

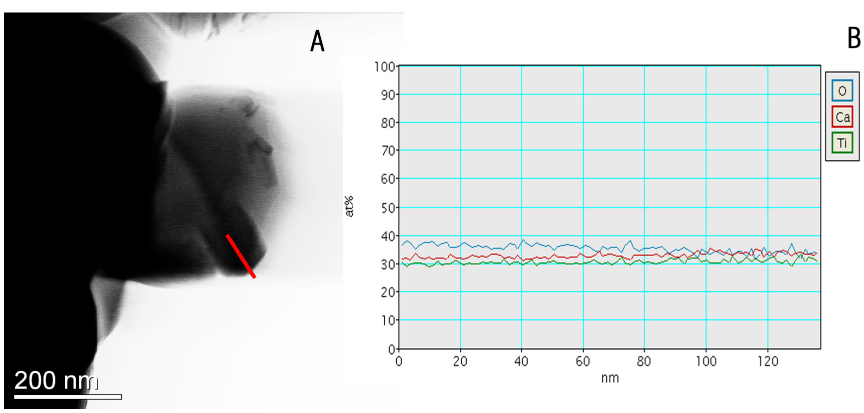

Fig. 2. (a) TEM micrograph of $CaTiO_3$:Pr sample with 3% Ca excess treated at 1400 °C. The line indicates the scan for EDS (Fig. 2(b)). (b) EDS line scan showing the elemental composition of $CaTiO_3$:Pr sample with 3% Ca excess treated at 1400 °C.

#160080 - $15.00 USD Received 19 Dec 2011; revised 1 Mar 2012; accepted 2 Mar 2012; published 7 Mar 2012

The excitation and emission spectra of samples with different Ca excess and thermal treatments can be observed in Fig. 3. The emission spectra are dominated by the red emission at 612 nm, which corresponds to the transition for $^1D_2$ to $^3H_4$ ground state. The excitation spectra present three bands, which are in agreement with previously reports in bibliography [12]. The A band (~330 nm) presents no changes in the intensity, while B (~360 nm) and C (~280 nm) exhibit clear changes in the relative intensities. Band B was reported to change the intensity with thermal treatment, which is in agreement with the observations in Fig. 3.

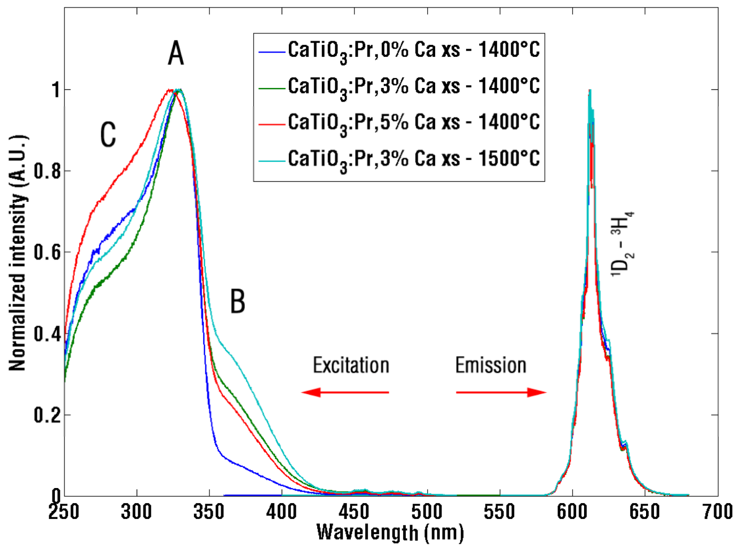

Fig. 3. Excitation and emission spectra of $CaTiO_3$:Pr samples with different Ca excess and treated different temperatures.

The persistent luminescence of the stoichiometric $CaTiO_3$:Pr samples treated at different temperatures is shown in Fig. 4. The persistent luminescence decay time exhibits an increase with the temperature of thermal treatment. This can be related to the reduction of non-radiative recombination centers and the efficient charge transport from traps to the emission centers as previously reported for nanoparticles treated at different temperatures [17].

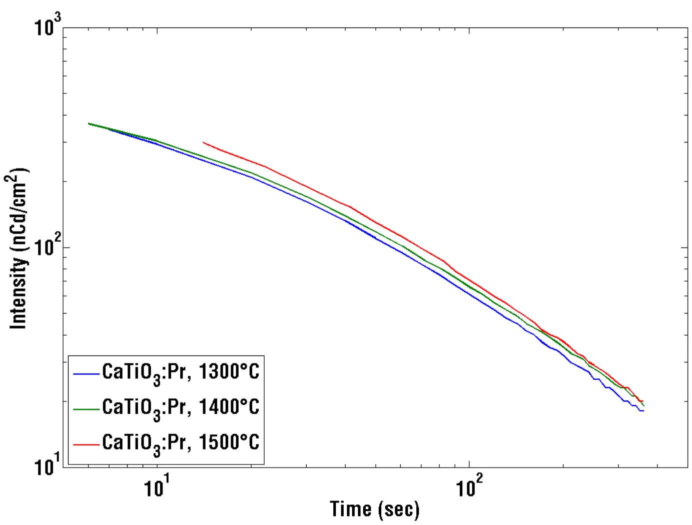

Fig. 4. Persistent luminescence decay of $CaTiO_3$:Pr stoichiometric samples treated at different temperatures.

#160080 - $15.00 USD Received 19 Dec 2011; revised 1 Mar 2012; accepted 2 Mar 2012; published 7 Mar 2012

The persistent luminescence decay of the samples with Ca excess treated at 1400 °C is shown in Fig. 5 and illustrates that all samples with Ca excess exhibit longer decay time than the stoichiometric one. As previously explained, the incorporation of CaO defects in the $CaTiO_3$ structure can induce the formation of oxygen vacancies [20] which can act as electron traps and increase the decay time in the persistent luminescence [12]. Remarkable is the maximum decay time at 3% of Ca excess.

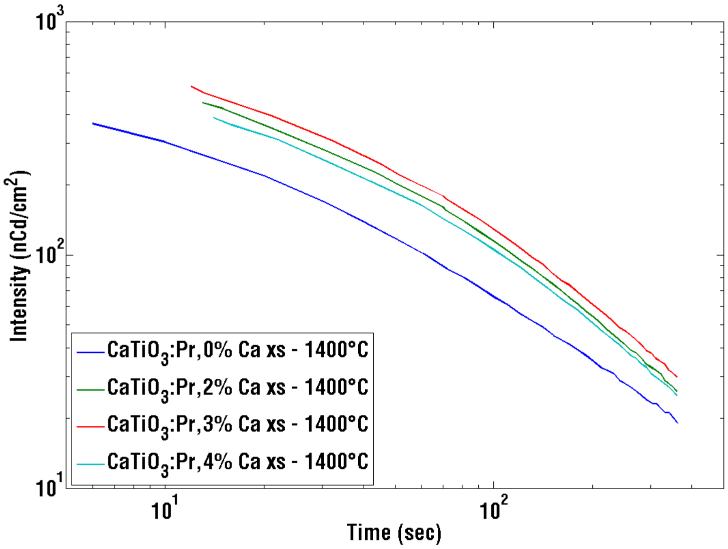

Fig. 5. Persistent luminescence decay of $CaTiO_3$:Pr samples with different Ca excess treated at 1400 °C.

It was reported that the substitution of Ba in $BaTiO_3$:Pr with trivalent ions (e.g. Al, Ga, Sc) has a strong influence on the luminescence intensity [26]. According to the mechanism presented, the substitution of trivalent ions located in the Ti sites close to Pr compensates the charge imbalance caused by the substitution of Ca by Pr. This indicates that a charge imbalance close to Pr ions reduces the luminescence intensity. In our case, the introduction of CaO excess would generate oxygen vacancies [20]. Low concentration of these defects act as traps, increasing the persistent luminescence decay time, but as the density of oxygen vacancies increases, these defects generate a charge imbalance and decrease the decay time.

The comparison of samples treated at 1500 °C show a different behavior in contrast to the group of samples treated at 1400 °C (Fig. 6). According to the observations in the XRD patterns (Fig. 1(c)), the Ca excess was segregated in the form of RP phases. The different decay time between the stoichiometric and non-stoichiometric samples suggest that some small amounts of Ca remains soluble in the matrix. This remaining amount of Ca in the matrix should be constant in the non-stoichiometric samples due to the precipitation of RP phases. This is reflected in the persistent luminescence decay time measurements (Fig. 6). Samples with non-stoichiometric composition have all the same behavior, which is clearly different from the samples with stoichiometric composition.

#160080 - $15.00 USD Received 19 Dec 2011; revised 1 Mar 2012; accepted 2 Mar 2012; published 7 Mar 2012

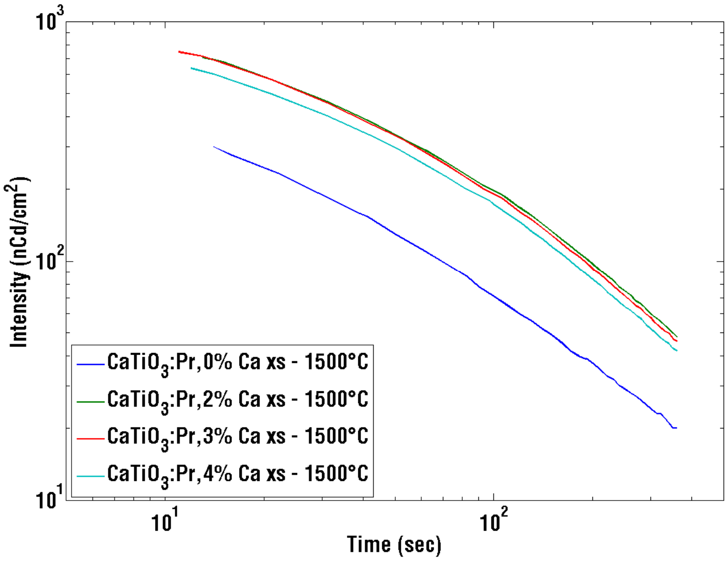

Fig. 6. Persistent luminescence decay of $CaTiO_3$:Pr samples with different Ca excess treated at 1500 °C.

The samples treated at 1500 °C showed the longest persistent luminescence of all samples despite that the remaining Ca excess in these samples is lower compared to samples treated at lower temperature. This indicates that a long persistent luminescence decay time is the consequence of more than one factor, which are in our case the higher thermal treatment and a Ca excess in the lattice. The time required to achieve the limit of light perception of the dark-adapted human eye of all the samples is summarized in Table 1.

Table 1. Time Required by Samples to Achieve Limit of Light Perception of the Dark-Adapted Human Eye

Sample	Decay time (sec)		
	1300 °C	*1400 °C*	*1500 °C*
0% Ca xs	201	221	231
2% Ca xs		311	453
3% Ca xs		341	446
4% Ca xs		296	415

To understand of the mechanism for luminescence decay, curves were plotted in log-log (Figs. 4–6) and hyperbolic. The lack of linearity of the curves indicates that there is not a simple single mechanism for de-excitation of charges in the system. To understand this mechanism, further characterizations should be performed.

4. Conclusions

Luminescent $Ca_{0.998+x}Pr_{0.002}TiO_{3+\delta}$ ($0.02 \leq x \leq 0.04$) samples with different afterglow properties were successfully prepared by solid state reactions with different thermal post treatments. Variations of the Ca content and thermal treatments allowed us to modify the defects which can act as traps and increase the decay time in persistent luminescence. The Ca excess showed to be soluble up to 4% in the form of local defects or isolated CaO slabs for the samples prepared at 1400 °C. The samples treated at 1500 °C revealed a defined concentration of Ca in the structure. A Ca content exceeding this concentration was segregated in form of RP phases. The Ca excess in the samples treated at 1400 °C showed that 3% is the best concentration for long time persistent luminescence. For the samples treated at 1500 °C, the constant Ca

#160080 - $15.00 USD Received 19 Dec 2011; revised 1 Mar 2012; accepted 2 Mar 2012; published 7 Mar 2012

concentration in the structure caused a similar decay time in the persistent luminescence. The samples treated at higher temperature showed the longest decay time despite of majority of Ca excess segregation from the $CaTiO_3$ lattice, showing that the small amount of remaining soluble CaO in the $CaTiO_3$ structure has a stronger effect on the luminescence than the higher concentrations in the samples treated at lower temperatures and indicating that the performance of long persistent luminescence pigments is the consequence of more than only one factor, e.g. thermal treatment and defect concentration in the lattice.

Acknowledgments

Financial support from Empa, LumiNova AG (Switzerland) and the Swiss Federal Office for Professional Education and Technology (KTI- Project Nr. 10640.1 PFIW-IW) is greatly acknowledged. The authors would also like to specially acknowledge and remember Paul Hug for his help along all these years.